Indian Journal of Chemical Technology
Vol. 5, January 1998, pp. 16-28

Correlation between structure and inhibition of organic compounds for acid corrosion of transition metals

M Jayalakshmi & V S Muralidharan
Central Electrochemical Research Institute , Karaikudi, 630 006, India

Received 11 March 1997; accepted 18 August 1997

In acid media, the corrosion inhibition offered by ethanol amines, benzoic acids, acetylinic alcohols for iron and nickel was investigated. These molecules adsorbed on the metal surface and offered inhibition. A correlation between inhibition and electronic configuration of the molecules was attempted. In benzoic acids, the anchoring group is the benzene ring and the electron delocalisation in the aromatic ring played a crucial role in the surface chelate formation. In the case of amines, the inhibition takes place due to adsorption via lone pair of electrons on the nitrogen atoms. Acetylinic alcohols offered inhibition by accepting electrons from the vacant '*d*'orbitals of the transition metals. On prolonged exposure in acid medium they form thick polymeric film on the metals thus offering inter-phase inhibition.

A large number of aliphatic and aromatic organic compounds, mainly those containing nitrogen, oxygen and sulphur atoms are found to cause a distinct decrease in corrosion rate of metals in acid media.These organic inhibitors may retard the corrosion processes either by specific adsorption leading to two dimensional protective layers. In order to understand the mechanism of inhibition, several attempts are made based on the correlation between the structure of organic compounds and their corrosion inhibition efficiency[1-8]. It is considered that the adsorption, electro nation, bond formation and allied mechanisms of interaction between the inhibitor and the metal can separately or together occur to bring about this inhibition. Development of quantitative structure- inhibition relationships (QSIR) have the longest history. Initially, pure empirical methods were employed validating the additivity principle for functional group contributions[9-11]. The attempt failed because electronic and steric interactions among the functional groups were not included. Subsequently, semi-empirical methods were employed. Initially, Bronsted acid-base correlation[12-28] is quite successful but steric terms are not considered. The dominant descriptor variable is the electronic contribution. Much more widely used QSIR is the linear free energy relationship and a very successful application of such relationship is the Hammett equation[28]. $\log \{K_x/K_h\} = P$,where $\{K_x/K_h\}$ is the ratio rate coefficients or equilibrium constants for a molecule with substituent x rather than h; P is a constant that depends upon the type of reaction being studied; and depends on the electronic characteristics of the derivative vs the parent molecule and may be calculated[30,31] or determined empirically[10,32]. The most successful semi empirical QSIR, is the Hansch correlation[33,34]. It is not so simple as that of Hammett correlation since it includes solubility/ dispersibility terms. However, the Hansch correlation is shown to be consistent for chemisorption of film forming inhibitors like *t*-cinnamaldehyde and derivatives on steel in concentrated HCl[35,36]. If the lipophilic/hydrophilic character of the molecule does not play a dominant role or such a situation does not arise, the Hammett equation holds good.

The paper deals with the inhibition of ethanol amines, acetylinic alcohols, benzoic acids in acid solutions. The inhibition of ethanol amines and acetylinic alcohols for acid corrosion of nickel and benzoic acids and acetylinic alcohols for acid corrosion of iron were studied. A uniform approach to understand the inhibition mechanism of these compounds by correlating structure with adsorption on the metal surface leading to intermediate chelate formation, which results in inhibition of corrosion is attempted.

Experimental Procedure

Materials

Swedish Pure Iron [99.95% Fe, 0.0056% Mn, 0.001% Si and 0.025% C] has been used. Pure nickel [99.9999%] supplied by Johnson Mathey, USA was used.

Chemicals

Benzoic acids (BA), salicylic acids (SA), ortho nitro benzoic acid (ONBA) and anthranilic acid [AA] of analytical grade were used in the concentration range of 5×10^{-3} to 2×10^{-3} M; 2-methyl-3 butyn-2-ol (MBO), propargyl alcohol (PA), 3-butyn-2-ol (BO) and 2-butyn-1,4-diol (BD) supplied by Aldrich , USA were used in the concentration range 1×10^{-4} to 10^{-2} M. Mono-, di- and -tri-ethanol amines of analytical grade supplied by Sarabhai Chemicals , India were used in the concentration of 5×10^{-2} M. Analytical grade reagents were used without further purification.

Three Electrode Cell

A three electrode cell with large platinum foil as auxiliary electrode and saturated Calomel Electrode as reference electrodes were used. The working electrode of iron [0.785 cm^2] and Nickel [0.196 cm^2] were used. The outer jacket of the cell was kept at desired temperature by circulating water from a thermostat. The solution under study were deoxygenated using purified hydrogen.

Weight change Method

Iron specimens of size [7.5×2.5 cm] and nickel specimens [5×1 cm] were polished and degreased with trichloro ethylene. They were weighed and suspended by using glass hooks without touching each other in 400 mL beakers kept in a thermostat [±0.1 K]. After specified periods of immersion they were removed, washed in tap water , dried and weighed. Triplicate experiments were done and the variation in weight change was ±5%.

Electrochemical methods

Galvanostatic polarisation—A constant current generator was used to apply different current steps. The electrode potential was followed with a digital volt meter. The steady value in potentials was measured and plotted against logarithmic current. Similarly potentio static polarisation was carried out by varying the applied potential using PAR potentio stat system.

Faradic impedance method—Sinusoidal current of various amplitudes were applied at the corrosion potential using a PAR impedance system { model no., 5206}. Impedance measurements were made in the frequency range of 0.1 to 1 kHz.

Small amplitude cyclic voltammetry (SACV)—The SACV experiments were carried out using ' CORROVIT' [Tacussel make] in conjunction with X-Y-t recorder.

Results and Discussion

Corrosion inhibition for iron

Benzoic acids—In the case of benzoic and salicylic acids, the inhibition efficiency generally decreased with temperature while for orthonitro benzoic acid and anthranilic acids, it increased with temperature. Antharanilic acid showed the highest efficiency in the range of 70-80% at the temperature of 363K (Table 1). Maximum efficiency was obtained within 30 min. There is a marginal decrease in efficiency with increase in immersion time. Concentration changes also had only marginal influence. In the case of orthonitro benzoic and antharanilic acids, the inhibition efficiency tends to decrease with concentration.

Table 1—Percentage inhibition efficiency for pure iron in 1.0 *N* sulphuric acid containing 0.01 M inhibitor

Inhibitor concentration 0.01 M	303 K				323 K				363 K			
	A	B	C	D	A	B	C	D	A	B	C	D
	38	24	40	33	30	23	14	15	12	15	16	3
BA	48	39	40	40	22	15	20	26	4	18	17	3
SA	9	9	4	5	—	18	30	46	46	55	56	59
ONBA	66	60	59	56	71	76	60	70	81	73	70	70

A - 30 min; B - 60 min; C - 90 min; D - 120 min; BA - Benzoic acid; SA - Salycylic acid; ONBA - Orthonitrobenzoic acid; AA - Antharanilic acid

The average activation energy for corrosion obtained from the calculated activation energies for 30 and 60 min of immersion time data, revealed that ortho nitro benzoic acid , Salicylic acid and antharanilic acid increased the energy of activation. The adsorption of benzoic acid, ortho nitro benzoic acid and salicylic acid is found to obey Langmuir isotherm [Fig. 1].

$$\theta/(1-\theta)=AC\exp[-\Delta G/RT] \quad \ldots (1)$$

At higher temperatures, this isotherm was found to be not applicable. Increase of temperature affected the rate of adsorption/desorption and if the rate of corrosion is faster than the rate of adsorption, there may be a decrease in inhibition with temperature. In the case of antharanilic acid, commonly used isotherms were found to be not applicable. The adsorbed unprotonated amino benzoic acid may lie flat on the corroding iron. This organic may displace some solvent molecules and the thermodynamics of it depends on the relative size of the inhibitor and solvent molecule. Other isotherms are:

$$\frac{\theta}{x(1-\theta)^x}=C_{org/55.4}\exp(-\Delta G_{ads}/RT) \quad \ldots (2)$$

$$\frac{\theta}{(1-\theta)^x}=\left(\frac{\theta+x(1-\theta)}{x^x}\right) \quad \ldots (3)$$

$$=C_{org/55.4}\exp(-\Delta G_{ads}/RT)$$

where C_{org} is the concentration of inhibitor in the bulk of the solution[37-40]. The Eqs (2) and (3) represent the Flory Huggins isotherm and Bockeris Swinkles isotherm respectively. A plot of LHS of the above equations against concentration gives a straight line passing through origin for the most probable x value. Figs 2 and 3 give the best straight line for x=3. The free energy of adsorption obtained for antharanilic acid from Flory-Higgins and Bockris -Swinkle isotherms are −5.9 kcal/mol and −1.19 kcal/ mol respectively. ONBA showed poor inhibition efficiency in comparison with others. When compared with the values obtained in uninhibited sulphuric acid solution, the open circuit potentials for all the inhibitors remained in the noble direction. The shift in the noble direction indicated the interference of these inhibitors with the anodic process. There is no quantitative relation between % inhibition and shift of potential in noble direction. ONBA exhibited very high positive potentials compared to others (Table 2).

In the SACV, the E-I curves exhibited hysteresis between the forward and reverse sweep with exponential type decay. At the start of both the sweep directions, the degree of hysteresis is sensitive to sweep rate (v) and only at the lowest sweep rate, it is considered to be negligible[41]. The gradient I_h vs v plot at $v=0$ is

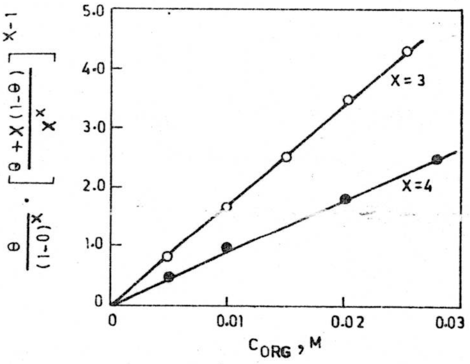

Fig. 2—Bockris-Swinkles adsorption isotherm for adsorption of anthranilic acid on iron from 1.0N H_2SO_4 solution at different x-values

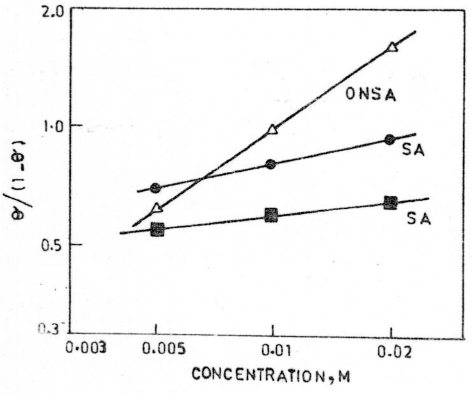

Fig. 1—logθ/(1−θ) vs log$c$ plot for benzoic orthonitrobenzoic and salicyclic acids at 303 K

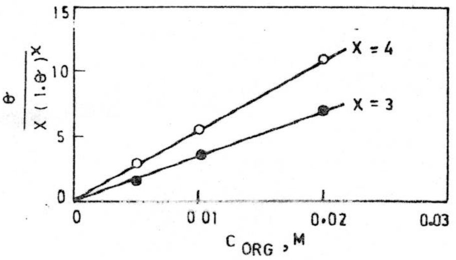

Fig. 3—Flory-Huggins adsorption isotherm for adsorption of anthranilic acid on iron from 1.0N H_2SO_4 at different x values

Table 2—Corrosion potentials (vs SCE) and percentage inhibition for pure iron at different concentrations of inhibitors in 1.0 *N* sulphuric acid solution 303 K

Concentration of inhibitor M	BA		ONBA		SA		AA	
	E_{corr}	% Inh	E_{corr}	% Inh	E_{cor}	% Inh	E_{corr}	% Inh
0.005	–500	41	–460	7	–490	41	–480	74
0.01	–530	38	–200	9	–490	48	–470	66
0.02	–470	60	–350	15	–480	49	–460	52

E_{corr} for pure iron in 1.0 *N* H_2SO_4 is –530 mV vs SCE
% Inhibitor values correspond to 30 min values
E_{corr} values are taken as soon as the specimen is immersed

$$\left(\frac{dI_h}{dv}\right)_{v\to 0} = \frac{2R_p^2 C_{dl}}{[R_p + R_s]^2} \qquad \ldots (4)$$

$$\left(\frac{dI_h}{dv}\right)_{v\to 0} = 2C_{dl} \text{ and} \qquad \ldots (5)$$

$$\left(\frac{d\eta}{di}\right)_{v\to 0} = R_p \qquad \ldots (6)$$

The electrode was polarised in the anodic direction upto 12.5mV and in the cathodic direction upto –12.5mV at different scan rates. The polarisation resistance values for ONBA are slightly less than in 1.0N uninhibited acid suggesting that ONBA is not an inhibitor. The R_p values for other acids suggests that the order of inhibition is AA>>SA>>BA [Table 3]. At the corroding electrode surface, these acids may perform the following functions: (i) Chemisorbing on the surface, (ii) Forming a more or less stable complex with a corrosion intermediates from the dissolution sequence, (iii) Formation of a complex with a final oxidative propensity The electron distribution through out the molecule will have some effect in the above three functions. A molecule with a great tendency for desorption may have small tendency for the formation of a surface complex. A molecule with a great affinity for lattice ion but a negligible tendency for long lived adsorption will function as an accelerator to corrosion. The scheme may be as follows:

$$Fe + OH^{--} \leftrightarrow FeOH_{ads} + e \qquad \ldots (7)$$

$$FeOH \leftrightarrow FeOH^{+} + e \qquad \ldots (8)$$

$$FeOH^{+} \leftrightarrow Fe^{2+} + e \qquad \ldots (9)$$

The dissolution phenomena would further lead to surface chelation with inhibitors as

$$FeOH_{ads} + n\, I \leftrightarrow Fe(OH\, I_n) \qquad \ldots (10)$$

Table 3—$R_p = (d\eta/di)_{\eta\to o}$ in ohms obtained from SACV method for pure iron into H_2SO_4 containing concentration of inhibitors at 303 K

Concentration of inhibitor of, M	ONBA	BA	SA	AA
0.005	2.8	10.0	10.0	20.0
0.01	3,0	10.0	10.0	20.0
0.02	3.0	16.6	13.3	20.20

R_p for pure iron in 1.0 *N* H_2SO_4 = 3.8 Ω

$$FeOH\, I_n \rightarrow (FeOH\, I_n)_{ads} \qquad \ldots (11)$$

$$(FeOH\, I_n)_{ads} \rightarrow FeOH\, I^{+}_{n} + e \qquad \ldots (12)$$

$$FeOH\, I^{+}_{n} \rightarrow FeI_n^{2+} + OH^{--} \qquad \ldots (13)$$

The inhibitor may interact or displace the solvent molecule or specifically adsorbed ion.

$$I + S \rightarrow I_{ads} + S \qquad \ldots (14)$$

If step (10) is the dominant mechanism for the production of chelate, then the formation of chelate would be enhanced by increased coverage of adsorbed inhibitor. If the surface coverage of FeOH leads to the subsequent formation of $FeOH^+$, then the chelation (step 10) must be faster, than step (8) or the adsorbed inhibitor concentration is to be more. If chelation forms by step (4) and the equilibrium are shifted to the right relative to each other and the stiochiometry of (8) i.e., whether *n*>1 will determine whether the inhibition will increase or decrease or remain constant.

Inhibition or adsorption is determined by the electron distribution in the anchoring group of the adsorbate. Benzene ring remains to be anchoring group in the case of benzoic acid. The anchoring ability is further increased by the hydroxy group substitution in SA and which improves delocalisation of electrons in the aromatic ring. Increasing inhibition with concentration suggest that chelation may take place with $(FeOH)_{ads}$. The observed adsorption pseudo capacitance 157.5 $\mu F\ cm^{-2}$ compared with uninhibited values suggests the roughing of the surface taking place during corrosion and the true area of the surface increased with time.

In the case of ONBA, the nitrogen group reduced the electron density in the aromatic ring and hence the tendency for adsorption. At 303 K, the inhibition offered at all concentrations is negligible. At higher temperatures and at all concentrations an inhibition efficiency around 50% and the formation of a black film on the surface suggest the inhibition by a non-porous product which is not observed at 303K. The reduction of ONBA to amino benzoic acid is expected at concentration >0.01M. A shift in corrosion potential to –200 mV and –350 mV compared with –460 mV (uninhibited acid) suggests that this compound reduced on iron. At higher temperatures, the reduction product adhered to the surface and brought about enhanced inhibition.

The presence of amino group in AA stabilises the electron density in the benzene ring. It is seen from the weight loss data that increase of concentration decreased the efficiency while temperature increased it. The energy of activation for corrosion was found to be high in presence of AA. It displaced three water molecules as evidenced by isotherms considered. The smaller negative values of free energy of adsorption suggested weak Van der Waal type of forces. The adsorption might be due to the six membered ring and nitrogen atom of the amino group. The adsorption of ring substituted anilines[41] on mercury was attached to the surface by π-bonds of the aromatic ring. Therefore, the electron density at nitrogen was directly coupled to the density at the aromatic ring. In this case adsorption was due to the interaction of π-electrons as evident by increasing inhibitor efficiency compared with BA. The greater inhibition was achieved only by the adsorption occurring parallel to the surface. The tendency to adsorb was greater than the formation of surface complex (step 14). The inhibition efficiency remaining constant with time suggests that adsorption was favoured. If chelation was favoured , the inhibition efficiency would increase with time of immersion. An inhibition efficiency of 60 to 80% suggests that the coverage by $FeOH_{ads}$ is low. Due to better inhibition, surface roughing cannot occur; hence a high value of adsorption pseudo capacitance of 145.8 µF cm^{-2} needs to be understood in terms of protonated amine or a proton. The presence of protonated amine or proton may affect the dielectric constant of the medium. The inhibition efficiency was due to unprotonated amino acids. The presence of ($FeOH_{ads}$) affected the area available for proton discharge in the cathodic reaction.

Acetylinic alcohols—Immersion time increased the inhibition efficiency and for a given concentration of inhibitor, BO offered highest inhibition followed by PA, BD = MBO (Table 4). Fig. 4 presents typical galvanostatic polarisation curves for pure iron in three different HCl solutions. The linear segments of the anodic and cathodic polarisation curves were extrapolated to corrosion potentials to obtain corrosion current. The anodic and cathodic Tafel slopes were found

Table 4—Effect of immersion time on the percentage inhibition efficiency in HCl containing 10^{-2} M inhibitor

Inhibitor	Time of immersion, min			
	30	45	60	90
PA	93	95	97	98
MBO	75	86	90	98
BO	98	95	96	98
BD	78	86	90	87

PA: Propagyl alcohol; MBO: 2 Methyl 3 Butyn-2-ol; BD: 2-Butyn-1:4 diol; BO: 3-Butyl-2-ol

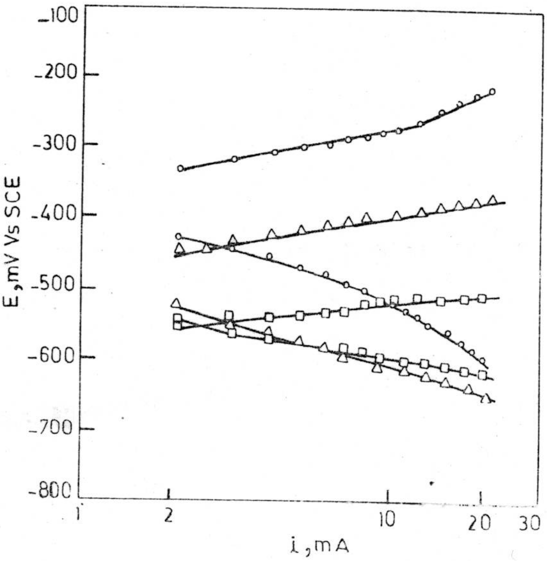

Fig. 4—Typical galvanostatic polarisastion curves for iron in three different hydrochloric acid solutions

to be 80 to 120 mV decade^{-1} respectively. These alcohols retard the rate of corrosion by increasing cathodic polarisation (Fig. 5). Acid concentration increased the inhibitor efficiency (Tabel 5) suggesting that the both H$^+$ ion and Cl$^-$ ions participate in the inhibition process. Concentration of inhibitor increased the efficiency for a given acid concentration. PA offered more inhibition in 1.0*N* acid while MBO offered highest inhibition in 5*N* and 8*N* acids; BD offered the least inhibition.

Adsorption of Cl$^-$ ion on the iron surface and subsequent complex formation was envisaged[42-45]. In sulphate solutions, the formation of iron complex had been suggested[46]. In similar lines, the anodic Tafel slope of 80 mV /decade under steady state polarisation may be due to the formation of hydroxo chloro iron complex. The Bockris mechanism for iron dissolution[46] is as follows

$$\mathrm{Fe} + \mathrm{OH}^{--} \leftrightarrow (\mathrm{FeOH})_{\mathrm{ads}} + \mathrm{e} \quad \ldots (15)$$

$$(\mathrm{FeOH}) \rightarrow \mathrm{FeOH}^+ + \mathrm{e}\ [\mathrm{rds}] \quad \ldots (16)$$

$$\mathrm{FeOH}^+ \leftrightarrow \mathrm{Fe}^{2+} + \mathrm{OH}^{--} \quad \ldots (17)$$

In addition, the reaction for the formation of the complex is assumed to be at equilibrium

$$\mathrm{Fe}^{2+} + m\,\mathrm{H_2O} + n\mathrm{Cl}^{--} \rightarrow [\mathrm{Fe(OH)}_m(\mathrm{Cl})_n]^{2-n-m} + m\mathrm{H}^+ \quad \ldots (18)$$

therefore, the over all reaction can be expressed by

$$\mathrm{Fe}^{2+} + \mathrm{m}\ \mathrm{H_2O} + n\ \mathrm{Cl}^{--} \leftrightarrow \mathrm{FeX} + n\mathrm{H}^+ + 2\mathrm{e} \quad \ldots (19)$$

At steady state, the H$^+$ and FeX produced must diffuse away continuously. Also the current is proportional to the diffusion rates of H$^+$ and FeX. The relation can be expressed by

$$i = -2\mathrm{FD}_{\mathrm{Fex}}\,[\mathrm{d}a_{\mathrm{Fex}}/\mathrm{d}x]_{x=0} = \frac{-2\mathrm{FD}_{\mathrm{H}^+}}{m}[\mathrm{d}a_{\mathrm{H}^+}/\mathrm{d}x]_{x=0} \quad \ldots (20)$$

Application of diffusion layer simplifies the situation and $(a_{\mathrm{H}^+})_{x=0}$ is assumed to be much larger than the activity of H$^+$ ion in the bulk of the solution.

$$i_{\mathrm{a}} = \left[\frac{2\mathrm{FD}_{\mathrm{H}^+}(a_{\mathrm{H}^+})_{x=0}}{m\delta}\right] = \left[\frac{2\mathrm{FD}_{\mathrm{Fex}}(a_{\mathrm{Fex}})_{x=0}}{\delta}\right] \quad \ldots (21)$$

where δ is the diffusion layer thickness; Insertion of $(a_{\mathrm{H}^+})_{x=0}$ thus obtained gives,

$$i_{\mathrm{a}}^2 = \frac{2\mathrm{FK}_{\mathrm{a}\rightarrow}\mathrm{D}_{\mathrm{H}^+}}{m\delta}\exp[(1+\beta)F\Delta\phi_{\mathrm{a}}/RT] \quad \ldots (22)$$

That is

$$i_{\mathrm{a}} = \left\{\frac{2\mathrm{FK}_{\mathrm{a}}D_{\mathrm{H}^+}}{m\delta}\exp(1+\beta)F\Delta\phi_{\mathrm{a}}/RT\right\}^{1/2} \quad \ldots (23)$$

Therefore

$$\{\mathrm{d}\Delta\phi_{\mathrm{a}}/\mathrm{d}\ \ln i_{\mathrm{a}}\} = 2RT/(1+\beta)F \quad \ldots (24)$$

Since the metal surface is covered by adsorbed Chlorocomplex, the positively charged alcohol may react as:

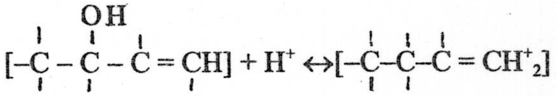

$$[-\underset{|}{\overset{|}{\mathrm{C}}}-\underset{|}{\overset{\overset{\mathrm{OH}}{|}}{\mathrm{C}}}-\overset{|}{\mathrm{C}}=\underset{|}{\mathrm{CH}}] + \mathrm{H}^+ \leftrightarrow [-\underset{|}{\overset{|}{\mathrm{C}}}-\underset{|}{\overset{|}{\mathrm{C}}}-\overset{|}{\mathrm{C}}=\mathrm{CH}^+_2]$$

... (25)

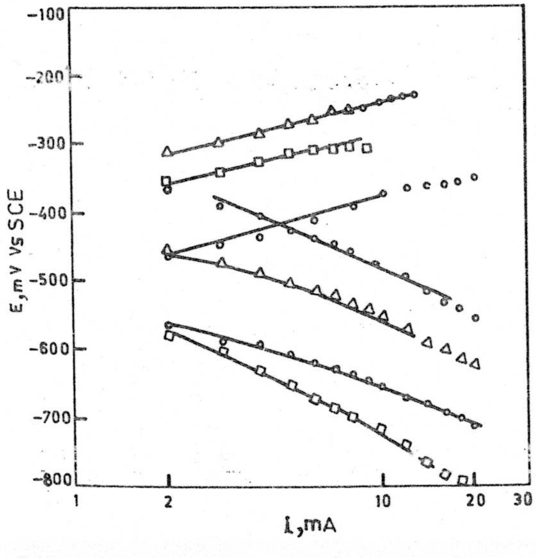

Fig. 5—Typical galvanostatic polarisation curves for pure iron in different concentrations of BD

Table 5—Influence of HCl concentration of the percentage inhibition efficiency for nickel in various concentration of inhibitors

Inhibitor	Concentration	% Inhibition		
	M	1.0 *N*	5.0 *N*	8.0 *N*
PA	10^{-4}	31	66	68
	10^{-3}	31	66	67
	10^{-2}	78	84	88
BD	10^{-4}	12	50	65
	10^{-3}	28	50	65
	10^{-2}	53	69	90
MBO	10^{-4}	25	67	67
	10^{-3}	37	72	—
	10^{-2}	58	87	89
BO	10^{-4}	42	59	59
	10^{-3}	42	65	65
	10^{-2}	50	70	70

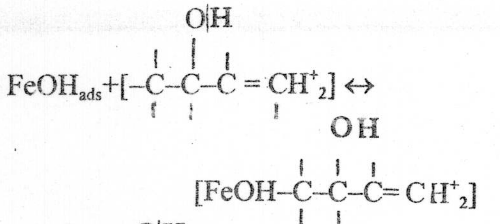

$$\mathrm{FeOH_{ads}}+[-\mathrm{C}-\overset{\mathrm{OH}}{\mathrm{C}}-\mathrm{C}=\mathrm{CH^{+}_{2}}]\leftrightarrow [\mathrm{FeOH}-\mathrm{C}-\overset{\mathrm{OH}}{\mathrm{C}}-\mathrm{C}=\mathrm{CH^{+}_{2}}] \quad \ldots (26)$$

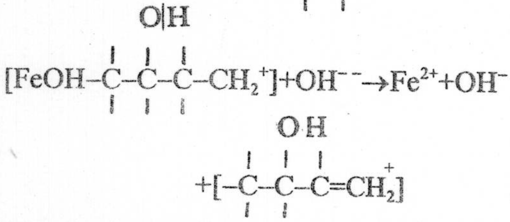

$$[\mathrm{FeOH}-\mathrm{C}-\overset{\mathrm{OH}}{\mathrm{C}}-\mathrm{C}-\mathrm{CH_2^{+}}]+\mathrm{OH^{--}}\rightarrow \mathrm{Fe^{2+}}+\mathrm{OH^{-}}+[-\mathrm{C}-\overset{\mathrm{OH}}{\mathrm{C}}-\mathrm{C}=\overset{+}{\mathrm{CH_2}}] \quad \ldots (27)$$

The formation of Chlorohydroxy iron complex is not favoured as the production of Fe^{2+} ions is hindered .The observed Tafel slope of 80 mV/ decade confirms this. This monomeric inhibitor molecule can undergo polymerisation so that a polymeric two dimensional system is formed which lightly adheres to the metal. In the case of BO and PA, the polarisation of the triple bond is stabilised first by a non-classical carbonium ion and then by a keto configuration which is known to complex with $FeOH_{ads}$. The terminal carbon - carbon triple bond stabilises π-electron interaction. In the case of BD, the non-terminal carbon-carbon triple bond does not favour π-bond interaction because of steric hinderance.

Corrosion inhibitors for nickel

Ethanol amines—Potentiostatic experiments were carried out after immersing the electrode in the solution under study and the open circuit potential reached a steady value. Corrosion currents were obtained by the extrapolation of anodic and cathodic Tafel lines to the corrosion potential. In all experiments, the anodic Tafel line extrapolation gave a higher corrosion current compared with the cathodic Tafel line extrapolation method. The corrosion currents obtained by anodic Tafel line extrapolation were used for analysis. The anodic and cathodic Tafel slopes were unaltered in presence of inhibitors in the concentration studied.

Table 6—Energy of activation and percentage inhibition for corrosion of nickel

Solution	% Inhibition at 303 K	ΔE kcal/mol
1.0 N H_2SO_4	—	−5.5
1.0 N H_2SO_4 + 0.05 M MEA	73	−9.1
1.0 N H_2SO_4 + 0.05 M DEA	40	−6.9
1.0 N H_2SO_4 + 0.05 M TEA	33	−7.1

MEA: Monoethanol amine, DEA: Diethanol amine, TEA: Triethanol amine

The inhibitor efficiency has been calculated for monoethanolamine[MEA] diethanolamine [DEA] and triethanol amine [TEA] from the corrosion currents.

$$\%\text{efficiency} = \{I_{corr}-I'_{corr}\} / I_{corr}\times 100$$

where I_{corr}, I'_{corr} are the corrosion rates in absence and presence of the inhibitors respectively.

MEA exhibited more inhibition than DEA and TEA at 303K and above. All three raised the energy of activation and MEA was found to raise it more when compared with DEA and TEA [Table 6]. This suggests that these amines may either participate in the electrode process or may change the potential difference of the metal/solution interface by adsorption. Since there is no change in the anodic and cathodic Tafel slopes in presence of these amines, inhibition may be due to the adsorption , Langmuirian type, which changes the interfacial potential difference (Fig. 6). Temperature rise caused an increase in corrosion but there is no definite relation between inhibition and concentration at temperature >303K.

Adsorption depends upon molecular size, shape, charge distribution, deform ability of the surface

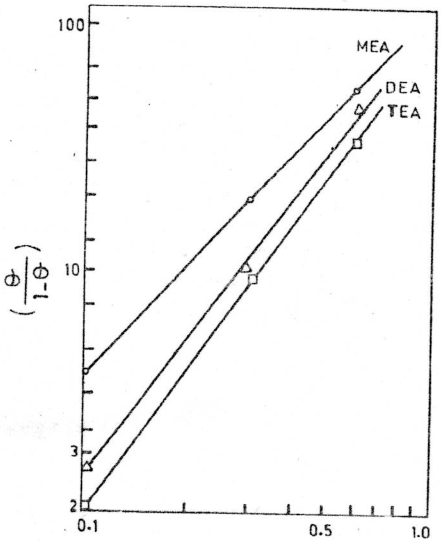

Fig. 6—Typical plot of log(θ/1−θ)) vs log*c* for all ethanolamines for Nickel in 1.0*N* H_2SO_4 at 303 K

active groups as well as charge on the metal undergoing corrosion[43]. Owing to the acidity of the medium, the amines may exist in the protonated form. The stability of the protonated form increased with the electron density on the nitrogen atom. MEA exhibits higher inhibition as it enhances the formation of the protonated species. In DEA and TEA, due to the inductive effect the electron density on the nitrogen atom has been decreased and the formation of the protonated species has been slowed down. Since Ethanol amines have more than one centre viz., nitrogen and oxygen for electron donation, the participation of the lone pair of oxygen is also possible. But all the lone pairs of electrons on oxygen atoms may not come closer to the metal, as the size of the molecule hinders adsorption. Though DEA and TEA have more oxygen atoms, their participation is restricted due to steric hindrance.

Acetylinic alcohols—Galvanostatic and potentiostatic methods gave nearly the same value in 1.0*N* and 10.0*N* acid solutions. There is very little deviation in 2*N* and 5*N* acids. Inhibition

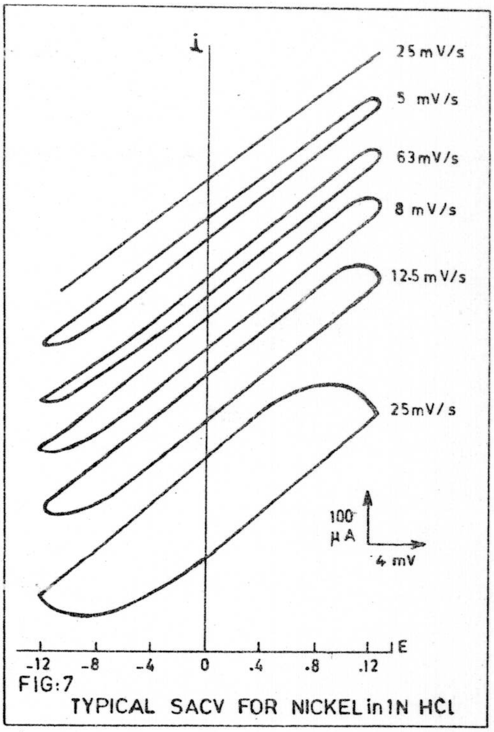

Fig. 7—Typical SACV for the corrosion of nickel in 1.0*N* HCl at different sweep rates

Table 7—Comparison of percentage inhibition efficiencies obtained from different methods

	Weight loss method	Impedance method	Galvanostatic method	Potentiostatic method	SALV from
1.0 *N* Acid + 0.01 M inh					
PA	83	95	95	95	50
MBO	75	96	87	86	53
BO	50	98	91	92	53
BD	65	87	86	86	27
2.0 *N* Acid + 0.01 M inh					
PA	85	—	97	97	43
MBO	—	—	90	96	36
BO	97	—	92	91	20
BD	72	—	92	21	—
3.0 *N* Acid + 0.01 M inh					
PA	92	95	92	94	76
MBO	97	80	76	96	81
BO	85	87	93	88	80
BD	—	—	89	96	77
4.0 *N* Acid + 0.01 M inh					
PA	100	98	89	87	69
MBO	60	97	93	97	41
BO	98	94	87	90	41
BD	90	66	93	90	46

efficiencies from weight loss method showed either the same or nearly 10% of the electrochemical methods. Impedance measurements (Fig. 7) gave nearly the same value as obtained by steady state electrochemical methods (Table 7).

The activation energy obtained for corrosion increased by acid concentration suggesting that both hydrogen and chloride ions favour corrosion. In presence of these alcohols, these increased (Table 8).

The dissolution of Nickel takes place as follows:

$$Ni + Cl^{--} \leftrightarrow NiCl_{ads} + e \quad \dots (28)$$

$$NiCl_{ads} + H^{+} \rightarrow NiCl\ H^{+} \quad \dots (29)$$

$$NiCl\ H^{+} + Cl^{--} \leftrightarrow Ni^{2+} + 2Cl^{-} + H^{+} \quad \dots (30)$$

with $NiCl_{ads}$ obeying Langmuir isotherm. The observed Tafel Slope of 60±10 mV suggested that

$$NiCl_{ads} + H^{+} \rightarrow NiCl\ H^{+} \quad \dots (31)$$

is the slow step. The rate expression may be written as

$$i_a = K_a\,(H^{+})\,(Cl^{-})(exp) - F\Delta\phi_a/RT \quad \dots (32)$$

where $\Delta\phi_0$ is the interfacial potential difference. In the hydrogen evolution reaction, the rate determining step is

$$H^{+} + e \rightarrow H \quad \dots (33)$$

corresponding to a Tafel slope of 135 mV. Both the rate determining steps involve the participation of [H^+] ions. A decrease of both nickel and hydrogen ions would result in a decrease in the corrosion rate of the two reactions. Hydrogen evolution reaction has a higher Tafel slope and can control corrosion by its low exchange current density.

Table 8—ActI, vation energies for corrosion of nickel (kcal/Mol) obtained with different concentration of HCl and 0.01 M concentration of inhibitors

System	Weight loss method		
	1.0 *N* HCl	5.0 *N* HCl	10.0 *N* HCl
Pure acid	−19.84	−14.72	−10.46
PA	−28.8	−22.80	−43.42
MBO	−30.0	—	−25.72
BO	−21.72	—	−23.41
BD	−28.14	−15.20	−26.72

In presence of alcohols the observed Tafel slope of 40 mV suggests that the rate determining step is changed. Cathodic Tafel slopes remained same or enhanced in presence of inhibitors suggesting that hydrogen evolution reaction is not affected considerably. In 10.0*N* acid solutions, the presence of alcohols had no effect except in the case of BO and BD (Table 9). This needs discussion. Since the metal surface is covered by adsorbed complex , the protonated positively charged alcohols may react as,

$$Ni + Cl^{--} \leftrightarrow NiCl_{ads} + e \quad \dots (34)$$

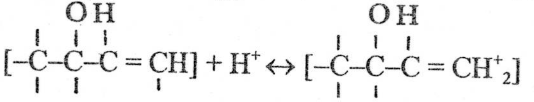

$$[-C-\overset{OH}{C}-C=CH]+H^{+}\leftrightarrow[-C-\overset{OH}{C}-C=CH^{+}_{2}] \quad \dots (35)$$

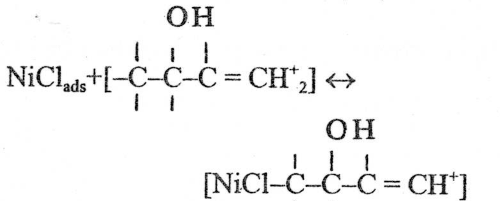

$$NiCl_{ads}+[-C-\overset{OH}{C}-C=CH^{+}_{2}]\leftrightarrow[NiCl-C-\overset{OH}{C}-C=CH^{+}] \quad \dots (36)$$

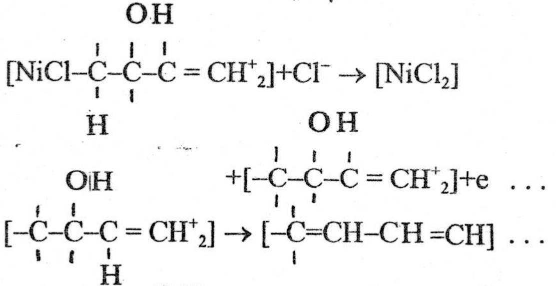

$$[NiCl-\underset{H}{C}-\overset{OH}{C}-C=CH^{+}_{2}]+Cl^{-}\rightarrow[NiCl_{2}]+[-C-\overset{OH}{C}-C=CH^{+}_{2}]+e \quad \dots (37)$$

$$[-C-\overset{OH}{C}-\underset{H}{C}=CH^{+}_{2}]\rightarrow[-C=CH-CH=CH] \quad \dots (38)$$

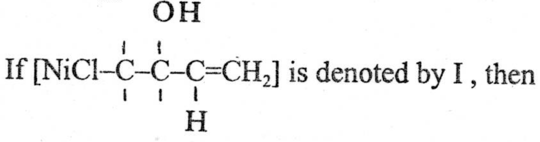

If $[NiCl-C-\overset{OH}{C}-\underset{H}{C}=CH_{2}]$ is denoted by I , then

$$\text{then } i_a = K_1K_2K_3k_4[I][Cl]\ \exp\ (1+\beta)F\phi/RT \quad \dots (39)$$

Table 9—Influence of inhibitors on the tafel slopes values obtained from galvanostatic measurement

Inhibitor	1.0 *N* HCl		2.0 *N* HCl		5.0 *N* HCl		10.0 *N* HCl	
0.01M	Anodic	Cathodic	Anodic	Cathodic	Anodic	Cathodic	Anodic	Cathodic
Acid	70	140	70	150	60	130	85	100
PA	30	120	30	110	40	140	85	130
MBO	40	110	30	100	40	140	80	100
BO	40	140	40	120	40	140	40	90
BD	40	120	40	120	40	120	70	90

This suggests an anodic Tafel slope of 40mV. The formation of Chloro complex is not favoured in presence of alcohols.

Alkyl chain and hydro phobicity—Adsorption of alcohols on the metal may be as follows:

(i) Chemisorption either by donation of electrons from the triple bond to the vacant *d* orbitals, or (ii) accepting electrons from the *d* orbitals to anti bonding orbitals of the triple bond, or (iii) both by electron and back electron donation.

In strong acid solutions, hydroxyl group of these alkynols can be thought to act just as electron withdrawing group in the molecule because it combines with proton in the acid forming Oxonium ions. Therefore, hydroxyl groups attached to alpha carbon of the triple bond should have stronger electron withdrawing property than that attached to carbon atom reducing electron density of the triple bond within the molecule. Greater is the decrease of electron density more adsorption by back donation on the surface and it is expected that adsorption by back donation inhibits mainly the cathodic reaction on Nickel.

The alcohols offer inhibition by adsorption, forming positively charged species, interaction of these species with adsorbed NiCl to form a positively charged barrier layer. These positively barrier layer prevents the approach of H^+ ions near the surface reduces the exchange current density of h.e.r. This reduction in exchange current density is responsible for the reduction in corrosion.

Unified mechanism of corrosion inhibition

Organic chemical compounds inhibit corrosion by adsorbing at the metal solution interface. The principal types are electrostatic adsorption, chemisorption and adsorption resulting π-bond interaction with the metal.

Electrostatic adsorption results from the coulombic interactions between the electric field at the outer Helmholtz plane (ψ-potential) of the double layer that exists on a metal-solution interface and the electric charge on certain inhibitor molecules. This adsorption depends on the zero charge potential of the metal, polarisability of anions and the electrical properties of the organic surface active molecules.

The stability of the protonated form of ethanol amines increased with the electron density on the Nitrogen atom. Monoethanolamine exhibited higher inhibition as it enhanced the formation of the protonated species. In di-tri ethanol amines, due to the inductive effect, the electron density on the nitrogen atom has been decreased and the formation of the protonated species has been slowed down. The lone pairs of electrons on oxygen atoms may not come closer to the metal as the size of the molecule hinders adsorption. Though di- and tri-ethanol amines have more oxygen atoms, their participation is restricted due to steric hindrance.

Chemisorption of an organic molecule on a metal in a corrosion medium involves the displacement of water molecules from the metal surface and the eventual charge sharing or even actual charge transfer or change sharing. The molecular structure, mode of adsorption and chemical nature of the "anchoring' inorganic group determines the efficiency of inhibition. The chemical bonding was discussed in terms of the Lewis acid base theory, the charge transfer theory, the extent of π-character of the electrons. The formation of quasi surface compounds or surface complexes is subjected to the spatial arrangement but it is evident they should be only one layer thick. Inhibition was found to increase when multi site association with the metal occurs.

In order to understand the role of acetylinic alcohols in affecting the hydrogen evolution reaction, the cathodic polarisation curves obtained

Table 10—Hydrogen evolution reaction - comparison of reduction in exchange current density for hydrogen evolution and inhibition efficiency in 10.0 *N* HCl

System	PA		BO		MBO		BD	
	θ	I, %	θ	I, %	θ	I, %	θ	I, %
10^{-5} M	0.89	74	0.86	74	0.97	86	0.76	86
10^{-4} M	0.92	78	0.90	76	0.98	88	—	85
10^{-3} M	0.95	84	0.89	74	0.98	93	0.83	90
10^{-2} M	0.97	90	0.89	90	0.99	98	0.89	93

$$\theta = \frac{i_{\mathrm{OH}} - i_{\mathrm{OH}}}{i_{\mathrm{OH}}}$$

in 10*N* HCl solutions were extrapolated to the reversible hydrogen evolution potential in these solutions (Table 10). The exchange current density was found to be 1.0×10^{-4} A/cm^2 and it was reduced by these alcohols.

$\Theta=[I_{O,H} - I'_{O,H}/ I_{O,H}$= reduction in exchange current density for h.e.r where $I_{O,H}$, $I'_{O,H}$ are the exchange current densities in presence and in absence of inhibitors. Increase of concentration of alcohols in 10.0*N* HCl solutions increased θ and % inhibition. There is no linear relationship between concentration and inhibition. Even 10*M* concentration offered 76% of the surface coverage and h.e.r may take place on the uncovered surface. Enhanced concentration help in the formation of positively charged protonated species.

A discussion on the structure of acetylinic alcohols and the inhibition efficiencies is presented below:

Propargyl alcohol has an hydroxy group in the alpha position to the acetylinic function. This favours the formation of non-classical carbonium ion intermediate and further to keto double bond configuration (Fig. 8). BO has both hydroxy and methyl group in the alpha position. The formation of carbonium ion is less favoured in BO compared to PA. MBO has one hydroxy and two methyl groups in the alpha position. BD is a symmetrical molecule with non-terminal triple bond. The stabilisation of π- electrons in the carbon-carbon triple bond is favoured as MBO> BO. PA>BD. Intra-molecular protonation is favoured in the order BO>PA>BD>MBO. MBO is a methyl substituted PA and increase in the alkyl chain imparts greater hydrophobicity to the interfacial layer, sequeezing out water molecules from the interface. These water molecules considerably reduce the protons near the interface. The subsitituted π-electrons of the terminal bond can come closer to the metal.

While correlating the structure with inhibition the following facts are to be considered.

(i) The π-electron density on the C≡C triple bond, (ii) Protonation at the lone pair of electrons on the oxygen atom, (iii) Keto- enol tautomerism, (iv) Intra molecular protonation through H bonding.

In the case of benzene molecule, the π-bonds

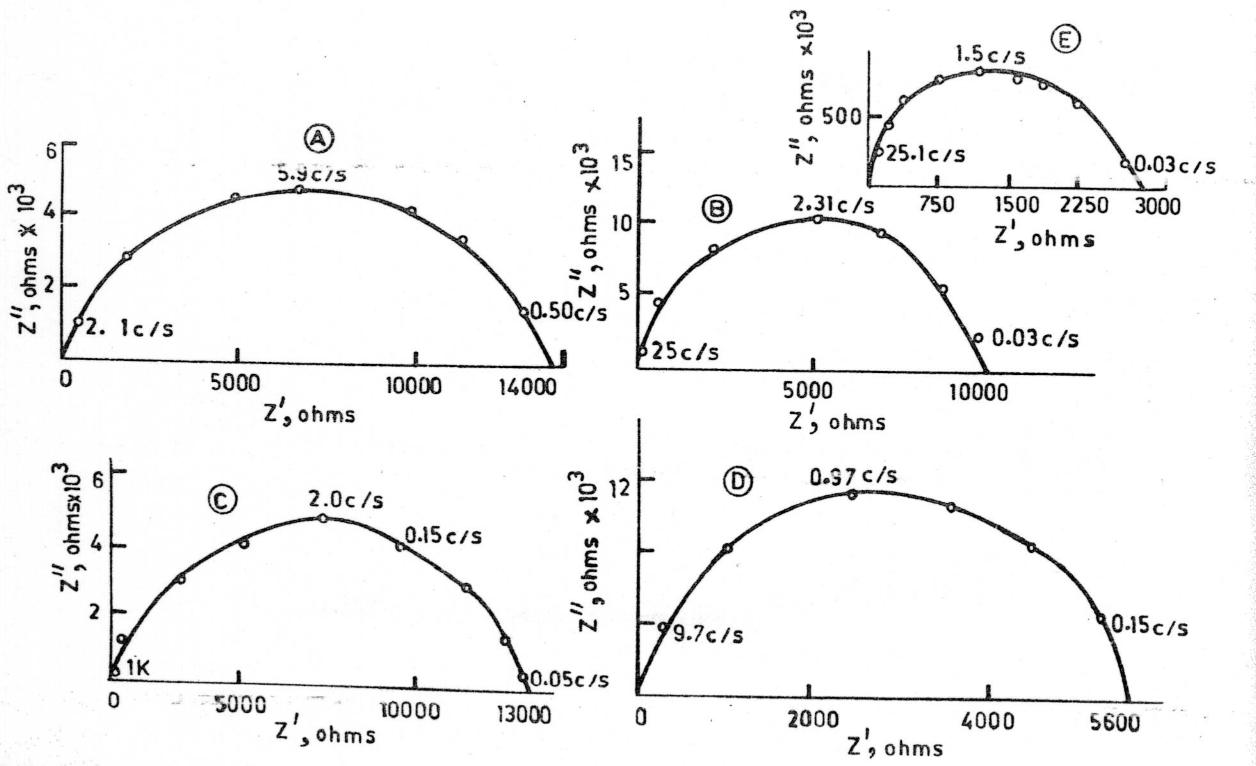

Fig. 8—Impedance diagram for the corrosion of nickel in 1.0*N* HCl containing 10^{-2}M alkynols at 303K: (a) No Inhibitor (b) PA (c) MBO (d) BO (e) BD

result also from SP, hybridization. Because of resonance, the main contribution to the bond character of benzene comes from bonds on Ortho form (Kekule form); the para form (Dewar form) is much weaker because the exchange energy between electron pairs, decrease rapidly with distance. Once a molecule gets Chemisorbed on the corroding surface, the kinetics of adsorption / desorption decides the formation of surface chelation .A molecule with a great affinity for lattice ion but a negligible tendency for long lived adsorption will favour dissolution. The precipitation of the solution soluble metal complex at the interface usually offer barrier protection. SA and ONBA chelated with $FeOH_{ads}$ intermediate favoured dissolution at their higher concentrations.

In the case of AA, the tendency to adsorb is greater than the formation of surface complex. The unprotonated amino group of the acid offered inhibition; however the inhibition is decided by the dynamic equilibrium between unprotonated and protonated amino acids. In the case of acetylinic molecule , an SP hybridisation produces two bonds at 180 and hence a linear molecule. Alkynols are chemisorbed on the metal surface either by donation of π-electrons of the triple bond to vacant *d* orbitals of the transition metal or by accepting the electrons from the π-anti bonding orbitals or by both. The hydrogen evolution on nickel was inhibited by these alcohols (80 to 99%). These suggest that these alkynols in strong acid solutions favour stronger electron withdrawing property from the π-antibonding orbitals of nickel. In presence of the higher surface coverage of these alkynols, the adsorbed hydrogen metal bond is strengthened. These impede both hydrogen evolution reaction and its permeation to the metal. Quantum chemical calculations on the adsorption of PA on iron confirmed that inhibitor acts as a strong electron acceptor from iron and the favourable mode of adsorption is via $C\equiv C^{49}$ triple bond.

Conclusion

Understanding the mechanism of corrosion inhibition offered by organic amines, acetylinic alcohols and benzoic acids by correlating their structure and electron delocalisation with the observed inhibition tendencies proves to be a technologically viable exercise. To screen the organic compounds that can be used as corrosion inhibitors such understanding is essential and worth while.

References

1 Hackerman N & Macrides A C, *Ind Eng Chem*, 46, (1954)523.
2 Donhaue F M & Ken Nobe, *J Electrochem Soc*, 114 (1967) 1012.
3 Hackerman N, *Eur symp on Met Corr Ferrara Campt,* Rend Univ, Ferrara, 89 (1961) 11.
4 Grigorev V P & Osipov O A, *Third International Conference on Metallic Corrosion*, Moscow, 158 (1966)1.
5 Grigorev V P & Kuzetsov V V, *Zashch Met*, 3, (1967) 178.
6 Grigorev V P & Ekilit VV, *Zashch Met*, 4 (1968) 31, 582.
7 Donhaue F M & ken Nobe, *J Electrochem Soc*, 112 (1965) 886.
8 Donhaue F M, Akiyama & Ken Nobe, *J Electrochem Soc*, 114 (1967) 1006.
9 Klopman S, *J Am Chem Soc*, 106 (1984) 7315.
10 Free S M & Wilson J W, *J Med chem* 7 (1964) 395.
11 Dupin P, De Savignac A & Lattes, *Werkst Korros,* 33 (1982) 203.
12 Horner L & Pliefke E, *Werkst Korros*, 33 (1982) 98.
13 Aromaki K, *Boshoku Gijutsu,* 33 (1983) 144, 33 (1984) 431, 35 (1986) 574, 36 (1987) 445.
14 Aramaki K & Nishihara H, *J Electrochem Soc*, 134 (1987) 1059.
15 Aramaki K, *Corros Eng,* 36 (1987) 409.
16 Aramaki K, Hagiwara M & Nishihara H, *J Electrochem Soc*, 103 (1987) 1896.
17 Aramaki K, Mochizuki T & Nishihara H, *J Electrochem Soc*, 135 (1988) 2427; 138 (1991) 394.
18 Aramaki K, Node Y & Nishihara H, *J Electrochem Soc,* 137 (1990) 1354.
19 Walters F H, *J Chem Educ,* 68 (1991) 29.
20 Pearson R G, *J Chem Educ* 45 (1968) 581, 643.
21 Pearson R G, *J Am Chem Soc,* 85 (1963) 3533.
22 Horner L, *Werkst Korros,* 24 (1973) 860.
23 Horner L & Schodel D, *Werkst Korros*, 25 (1974) 711.
24 Spinelli P, Fra tesi R & Roventi G, *Werks Korros,* 34 (1983) 161.
25 Yamaguchi M, Nishikara H & Aramaki K, *Corros Sci,* 36 (1983) 161.
26 Aramaki K, Tomihari M, Furuya S, Yamaguchi M & Nishikara H,*Corros Sci*, 36 (1994) 1133 .
27 Szklarska -Smia lowska Z, *Proc 7th Eur Symo on corrosion inhibitors,* Universita degli Studi di Ferrara Vol 1, (1991) 976.
28 Stair PC, *J Am Chem Soc,* 104 (1982) 4044.
29 Hine J, *Physical Organic Chemistry* (Mc Graw Hill, New York),1956, 69.
30 Vosta J, Eliasek J & Knizek P, *Corrosion*, 32 (1976) 183.
31 Reynolds W F *et al.*:, *J Am Chem Soc* 105 (1983) 378.

32 Singh I, *Corrosion*, 49 (1993) 473.

33 Hansch C & Fujita,*J Am Chem Soc*, 86 (1964) 1616.

34 Hansch C, *Ann Rep Med Chem (USA)*, 33 (1968) 348.

35 Growcock F B, *Corrosion*, 45 (1989) 1003.

36 Growcock FB, Frenier WW & Andereozzi, *Corrosion*, 45 (1989) 1007.

37 Flory P J, *J Chem Phy*, 10 (1942) 51.

38 Higgins M L, *Ann N Y Acad Sci*, 4 (1942) 31.

39 Dhar H P, Conway B E & Joshi, *Electrochem Acta*, 18 (1973) 789.

40 Bockris J OM & Swinkle D A J, *J Electrochem Soc*, 111 (1964) 736.

41 Macdonald D D, *J Electro Chem Soc*, 125 (1978) 1443.

42 Blomgren E & Bockris J O M, *J Phy Chem*, 63 (1959) 475.

43 Tedeschi R D & More G L, *I & EC Product Res Dev*, 9 (1970) 83.

44 Monroe R F, *Acetylinic derivatives as hydrochloric acid inhibitors*, AAAS Meeting Dec 28,1957.

45 Frenier WW, Lopp VR & Grancock, *Proc European Symposium on corrosion inhibitors*, Ann University, Ferrara, Italy, 1985.

46 Kurbanov F K & allaborgenov N D, Zasch Met, 15 (1979) 472.

47 Bengali A & KenNobe, *J Electrochem Soc*, 126 (1979) 1118.

48 Mirgaeva Z F, Kurbanov F K, Ikramov & Khamrabaeva Kh A, *J Appl Chem (USSR)*, 57 (1985) 2429.

49 Katej P, Vosta J, Pancir J & Hackerman N, *J Electrochem Soc*, 10 (1965) 679 .